

I. R. Baikov, A. R. Bergardt, V. K. Kedrinskii,
and E. I. Pal'chikov

UDC 534.222.2+532.528

This paper deals with some features of methods of recording nonstationary cavitation produced by intense pulsed loading of a liquid having a free boundary. Often, the processes include coalescence between individual cavitation bubbles and the formation of damage zones, whose structure resembles a foam. At certain tensile-stress intensities in the cavitation zones, one can get spalling phenomena [1]. However, the zone of intense cavitation is optically opaque, so it is impossible to examine the failure in the liquid at an early stage. The analysis is further complicated by the fact that the cavitation extends to a considerable volume of liquid in strong negative-pressure waves, whereas analogous processes in solids show the damage (spalling) zone localized near a certain plane, where the spalling surface occurs under appropriate conditions.

There are only a few papers on failure dynamics in liquids, which is due largely to the above features, but which is also dependent on our understanding of the failure effects. It is frequently assumed that the occurrence of a cavitation zone accompanying ultrasonic-wave propagation or focusing is an obvious sign that the continuity of the medium has failed and that certain strength properties have been lost. In such arguments it is inexplicitly assumed that a small tensile stress must be applied to the liquid in order to produce a discontinuity in the cavitation zone. It is obvious that the cavitation vanishes when the ultrasonic source is switched off and the liquid again becomes homogeneous. This is not observed in explosion experiments. In an underwater explosion, the brief tensile stresses (single pulse) produce not only a substantial cavitation cluster, but whose characteristic existence time considerably exceeds the negative-pressure duration, but also leads to the formation of a domed dispersal structure [1].

Various experimental studies are concerned with spalling failure mechanisms in solids. For example, in [2, 3] studies were made on the failure dynamics in polymethacrylate when a planar shock wave was reflected from a free surface. A laser method was used, which was based on light scattering by microcracks acting as nuclei for the spalling. The microcrack growth dynamics could be examined, and the failure stages in this polymer were examined, which indicated the failure mechanism in the microsecond range. No detailed studies have been made on the failure of liquids in this case. The present study may therefore be considered as dealing with failure in water under pulsed loading from the viewpoint of detailed mechanism discussion and the derivation of concrete quantitative information on the effects of the time and amplitude parameters of the negative pressure on the entire process.

We used the shock-tube method, which is particularly convenient as regards the production of a planar one-dimensional shock wave with adjustable parameters, whose interaction with the free surface of liquid results in a cluster.

Within this framework, we naturally have to consider the methods of recording the phenomena. A difference from the analogous case of failure in a solid is that the final result in a liquid cannot be established after the load has acted, since the liquid does not retain any cavitation damage. It is therefore necessary to record the characteristic parameters (bubble sizes and concentration) during the experiment itself. The usual method of high speed photography cannot give the necessary information for the reasons indicated above. It is therefore necessary to perform simultaneous recording of the cavitation by optical and x-ray methods, which should enable one to examine the dynamics of the external and internal cluster structures.

The experiments were performed with a cavitation shock tube, which was an ordinary three-section shock tube [4] split up by two diaphragms (Fig. 1). One of them d_1 separates the

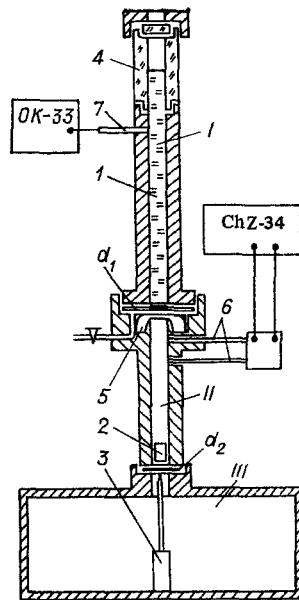


Fig. 1

working channel I containing the liquid 1 from the acceleration channel II, in which the striker piston 2 is accelerated in vacuum by compressed air. The second diaphragm d_2 separates the evacuated channel II containing the piston from the high-pressure chamber III containing compressed air. The chamber contains an electromagnet with needle 3 to provide forced failure of diaphragm d_2 to initiate the acceleration of piston 2. The working channel I contains the transparent section 4 providing optical recording of cluster growth near the free surface of the water. The same section is used in x-ray recording. Diaphragm d_1 is a metal disk of thickness 0.5 mm cemented to a Lavsan film with epoxide resin. Before the experiment, the air was evacuated from the acceleration part of a pressure of 10^2 Pa, and the piston is located in the lower part on the diaphragm d_2 . When the diaphragm fails, the piston is accelerated by the compressed air and strikes diaphragm d_1 . The resulting shock wave in the water is reflected from the free surface as a negative-pressure wave, which causes the continuity of the liquid to fail. To prevent damping of the piston impact by the air remaining in the channel directly in front of diaphragm d_1 , there is a special cavity 5 in the tube wall.

The shock-wave profile and parameters (amplitude and duration) and those of the negative-pressure wave are determined by the shape of the piston and its speed at the time of impact. The piston took the form of a vessel of diameter 30 mm and length 25 mm made of PTFE having an acoustic impedance close to that of water. Its speed was recorded by two optical fiber transducers 6, which operate from the reflection from the wall of the piston. The latter is accelerated over a section of length $L = 250$ mm by the virtually constant pressure difference Δp , which can be adjusted in the range $1-20 \times 10^5$ Pa. The speed u_0 at the instant of impact is defined by $u_0 = \sqrt{2\Delta pLS/m}$, and with mass $m = 20$ g and channel cross section $S = 7$ cm² may attain 170 m/sec. The stress amplitude in the shock wave can be calculated from formulas for the collision between two bodies in the acoustic approximation:

$$u = u_0 R_1 / (R_1 + R_2), \quad p = u R_2,$$

where u is the mass velocity of the liquid behind the shock wave front, p is the pressure amplitude behind the front, and R_1 and R_2 are the acoustic impedances of the piston and liquid correspondingly. Putting $R_1 \approx R_2$, we get that the apparatus enables one to vary the amplitude in water over the range $0.1-1.2 \times 10^8$ Pa. The design also enables one to provide pressure calibration. The pressure profile in the liquid is recorded by the piezotransducer 7 (Fig. 1) in the wall of the working part. The design is similar to that described in [5]. A typical pressure waveform is shown in Fig. 2 (beam 1). The pressure pulse is approximately square, amplitude 2.5×10^7 Pa and duration 70 μ sec.

PIR-100/240 x-ray equipment was used to examine the internal structure as the spectrum was suitable for use with a liquid under the above conditions: beam quantity energy 70 keV, maximum 200 keV, exposure dose in a single flash at 210 mm from the focus $\geq 120 \times 10^{-3}$ R, and pulse duration at half height 80 nsec.

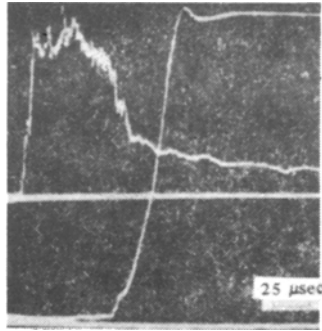


Fig. 2

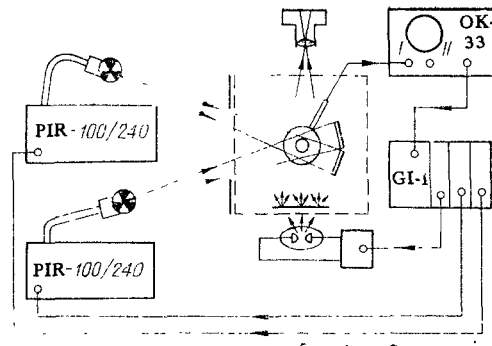


Fig. 3

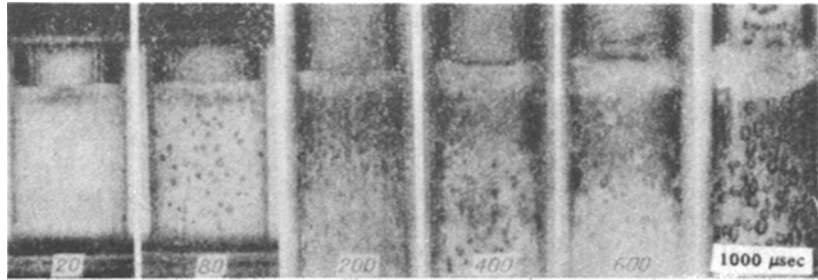


Fig. 4

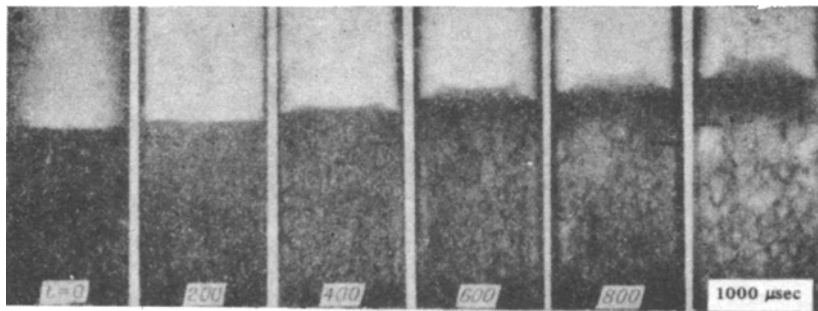


Fig. 5

Figure 3 shows the recording system. The signal from the piezotransducer near the diaphragm triggers the sweep in the OK-33 oscilloscope. At the same time, the oscilloscope passes a signal to the GI-1 pulse generator, which triggers the flash lamp and the x-ray equipment with the necessary delay. The flash lamp is installed to provide pulse illumination of the instantaneous state, and it gives a flash of duration 2 μ sec at half height, energy in a pulse not less than 1 J.

Figure 4 shows photographs of the cluster near the free surface. The bubbles begin to grow essentially behind the negative-pressure front. The cluster is separated from the free surface by a thin continuous water layer. At the same time as the cavitation occurs, a certain structure is formed at the free surface, which resembles a jet. This evidently occurs from a combination of capillary and cumulative effects, as well as because of the wall effect. The thickness of the continuous liquid layer increases as the bubbles grow, and the boundary between the cavitation region and this layer becomes more clear-cut. The later pictures do not enable one to consider the internal structure of the cluster at this stage because of the pronounced refraction and reflection at the gas-liquid boundary.

The x-ray pictures (Fig. 5) enable one to consider the cluster structure at the bubble coalescence stage. The bubbles are hardly distinguishable on the picture corresponding to 200 μ sec, but then the water-tube wall boundary becomes clear. The static frame ($t = 0$ sec) does not show this boundary. Bubble growth is evident in the later pictures, with the bubbles combining into a damage focus, which has a foam structure. The sizes of the

structures (cells) formed by bubble merging may be 5 mm or more. The x-ray pictures enable one to determine the instant when the failure focus forms and the size of it.

The internal structure in the surface jet is different from the external picture observed optically. While the optical pictures show a banded structure, which may be taken as a series of separation layers, the x-ray pictures indicate a continuous jet with a crater at the vertex.

Comparison of the optical and x-ray data indicates that recording in the optical range becomes ineffective at a certain stage in the accumulation of cavitation bubbles, since we lose information on the internal structure of the cavitating region. The x-ray pictures show that the failure zone is produced under these conditions at 200-300 μsec after the load is applied. The x-ray method enables one to detect density changes of 2-4% reliably, so one can say that the start of damage visible from the x-ray pictures corresponds to a bulk bubble concentration in the cluster of about 4%. At 800-1000 μsec one can see the structure of the damage focus and estimate the parameters. The bubble sizes are measured directly. One can photometer the x-ray pictures to establish the proportions of liquid and gaseous fractions in the cluster exactly. For example, the proportion of gaseous fraction is about 30% at 800 μsec .

The continuous layer of liquid at the free surface is produced on account of the response of the bubbles to the character and duration of the negative-pressure wave: In the reflection of a shock wave having an essentially square form, the layers of liquid close to the free surface are subject to tensile stresses of comparatively short duration. Virtually no cavitation occurs here, since the bubbles rapidly collapse after brief growth.

To monitor the profile of the shock wave emerging at the surface, we performed special measurements on the speed of the free surface using a condenser microphone. One of the plates in the planar capacitor was provided by a metallized Lavsan film of thickness 0.02 mm, while the other was a disk made of metallized glass-fiber material. The film was on the surface of the water, while the disk was 2 mm away. A potential of 100 V was applied to the disk through a resistor $r \sim 10^9 \Omega$. The value of r was chosen such that displacement of the capacitor plate for times up to 10^{-2} sec scarcely affected the charge on the latter.

The change in voltage ΔU on the capacitor was measured with a high-impedance follower circuit and was applied to input II of the OK-33 oscilloscope. This is related to the capacitor plate displacement x by

$$\Delta U = U_0 x / [h_0 + C(h_0 - x)],$$

where U_0 is the initial voltage, h_0 is the initial distance between the plates, and C is the ratio of the input capacitance of the follower and connecting cable to the condenser capacitance. Figure 2 shows the waveform (beam II). At the initial instant, the speed of the free surface is 32 m/sec (the speed of the piston at the instant of collision was 43 m/sec). The difference in the speeds of the free surface and piston at the time of collision is due in particular to the pulse being attenuated on propagating along the channel containing the water because of wall deformation. Subsequently, the surface speed decreases somewhat, but at 25 μsec it increases sharply to 30 m/sec. This relationship is evidently due to the vigorous bubble growth. The resulting cavitation region will affect the tail of the loading wave at the free surface.

Therefore, one can combine the optical and x-ray measurements with measurements of the pressure and free-surface motion to follow the dynamics of the internal and external structures of the liquid in negative-pressure waves, and one can estimate the proportion of the vapor-gas fraction and the size of the damage region.

We are indebted to E. I. Bichenkov and R. L. Rabinovich for substantial assistance in developing the apparatus used in the x-ray section.

LITERATURE CITED

1. V. K. Kedrinskii, "Surface effects in underwater explosions (review)," Zh. Prikl. Mekh. Tekh. Fiz., No. 4 (1978).
2. L. D. Volovets, N. A. Zlatin, and G. S. Pugachev, "The failure mechanisms in solids for lifetimes in the microsecond range," Pis'ma Zh. Tekh. Fiz., 4, No. 18 (1978).
3. L. D. Volovets, N. A. Zlatin, and G. S. Pugachev, "The production and growth of submicrocracks in polymethylmethacrylate on dynamic loading (spalling)," Pis'ma Zh. Tekh. Fiz., 4, No. 18 (1978).

4. M. I. Vorotnikova, V. K. Kedrinskii, and R. I. Soloukhin, "A shock tube for studying one-dimensional waves in a liquid", *Fiz. Goreniya Vzryva*, No. 1 (1965).
5. V. I. Zagorel'skii, N. N. Stolovich, and N. A. Fomin, "A pulse piezoelectric transducer with matched amplifier for measuring rapidly varying pressures," *Inzh.-Fiz. Zh.*, 42, No. 2 (1982).